Supporting Information

# All-solid-state Flexible Supercapacitors using Nanotube-reinforced Polypyrrole Hollowed Structures

*Hyungho Kwon, Dong jin Han and Byung Yang Lee**

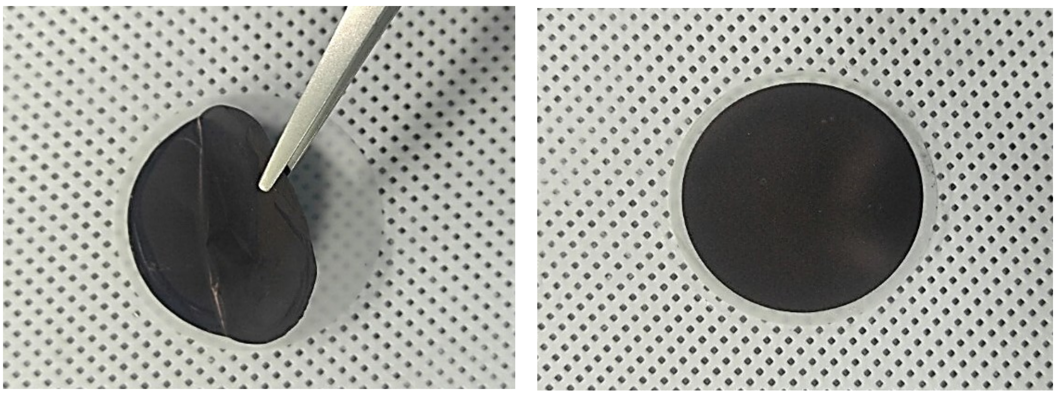

**Figure S1. Optical images of CNT/rGO films on AAO.** (a) CNT/rGO film (2 mg) on untreated AAO membrane and (b) on APTES-treated AAO membrane. It can be seen that the CNT/rGO film has much more stable adhesion on APTES-treated AAO membranes.

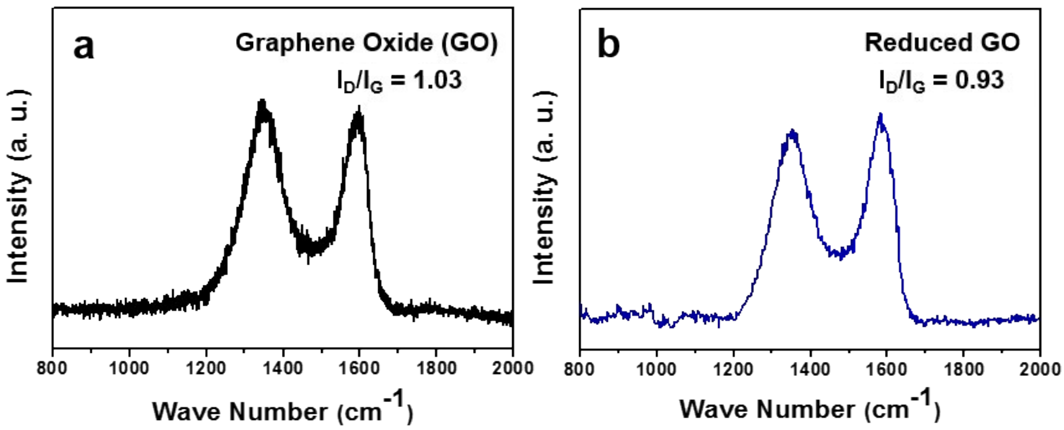


**Figure S2. Raman spectroscopy before and after graphene oxide reduction.** Raman spectroscopy images of (a) graphene oxide and (b) reduced graphene oxide by thermal annealing. After annealing, the $I_D/I_G$ ratio characterizing the structural disorder in graphenic materials decreased. This can be attributed to both the reduction of oxygenated functional groups and the partial restoration of the $sp^2$ network.[1]

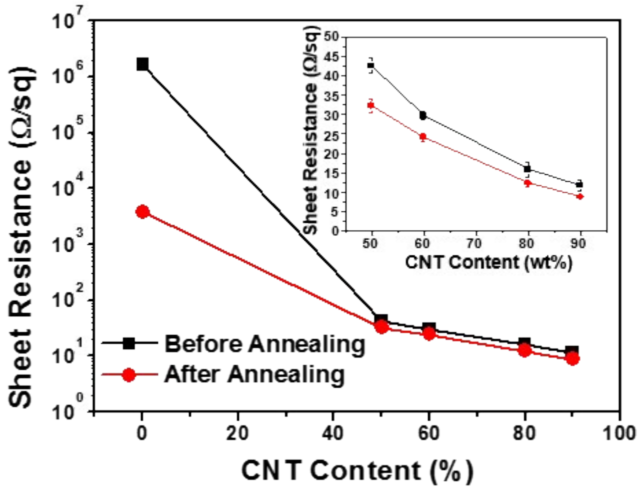


**Figure S3. Sheet resistance of CNT/rGO films (total mass of 2 mg) according to CNT content before/after thermal annealing.** There was a significant reduction in sheet resistance after annealing depending on the CNT content, which is similar to that reported by Huang, Zhen-Dong, et al.[2] For example, the sheet resistance decreased from $1.63 \times 10^6$ Ω/sq to $3.8 \times 10^3$ Ω/sq for 0 wt% CNT. For 90 wt% CNT, the sheet resistance dropped from 11.71 Ω/sq down to 8.8 Ω/sq after annealing. Inset shows the magnified view for low frequency data.

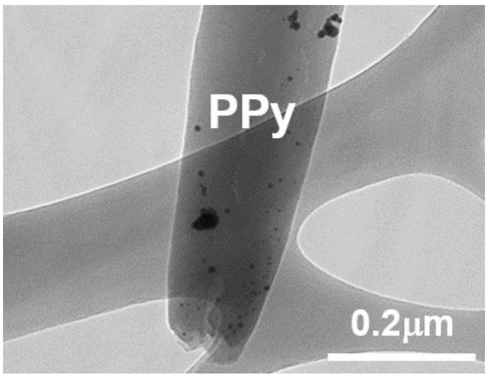


**Figure S4. Transmission electron microscope image of a PPy NW.**

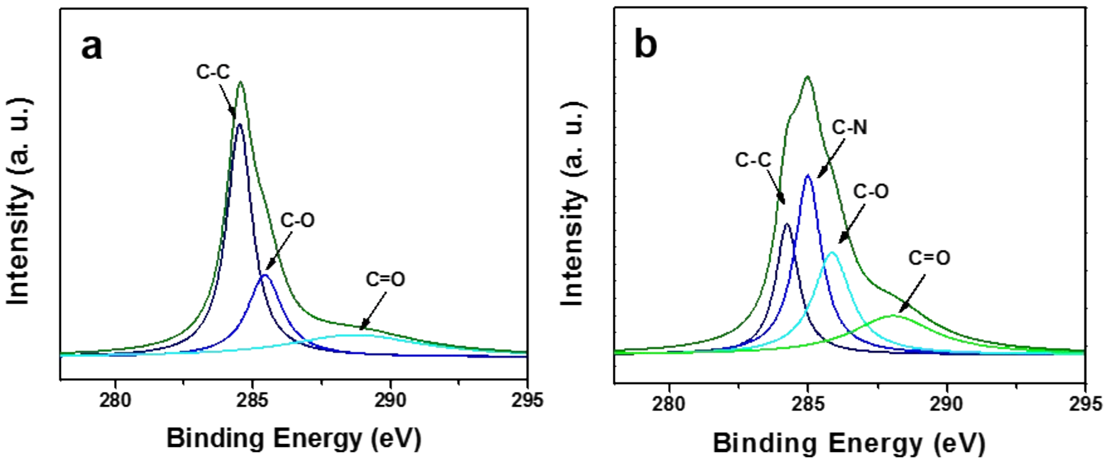


**Figure S5. XPS with high resolution C 1s spectra of (a) a CNT/rGO hybrid base and (b) PPy NW array films.**

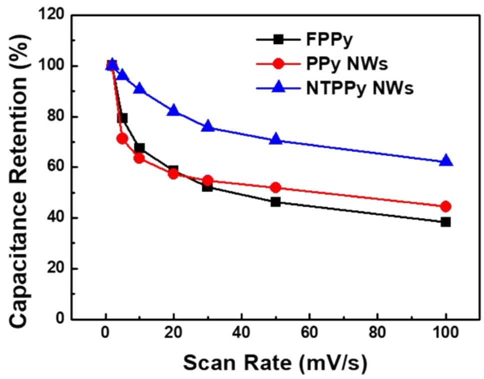


**Figure S6. Capacitance retention of FPPY, PPY NW array and NTPPy NW array films at various scan rates of 2 to 100 mV/s.** The retention values were extracted from the CV data in Figure 4b.

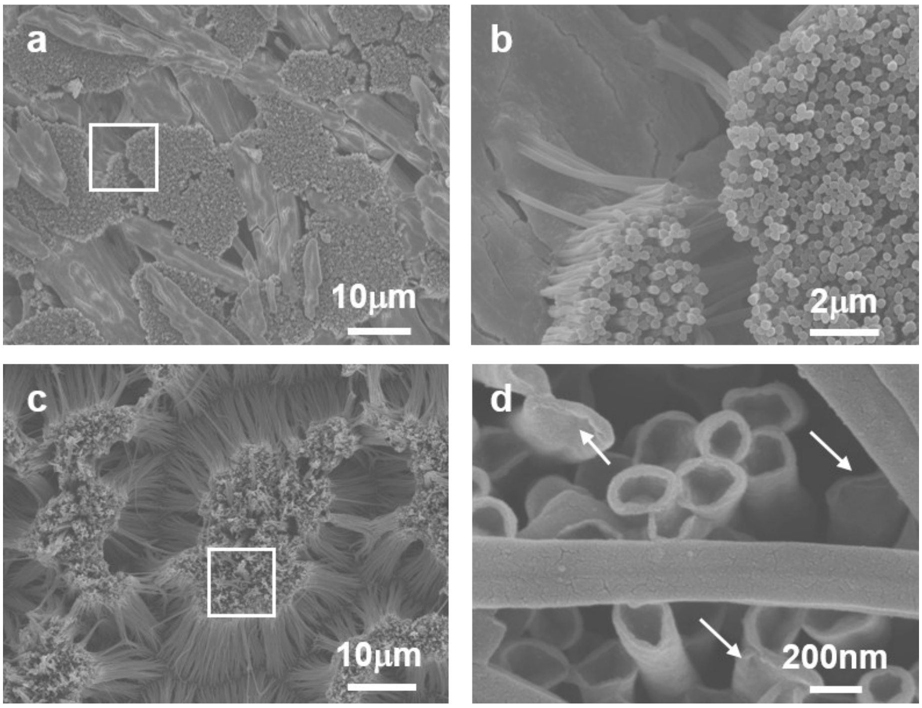


**Figure S7. Scanning electron microscope images of PPy NWs ((a) and (b)) and NTPPy NWs ((c) and (d)) after 3000 charge/discharge cycles.**

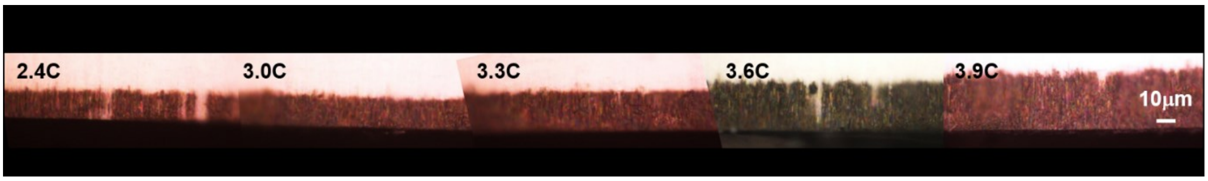


**Figure S8. Microscopic image of NTPPy NWs with different electrodeposition charges from 2.4 C to 3.9 C.**

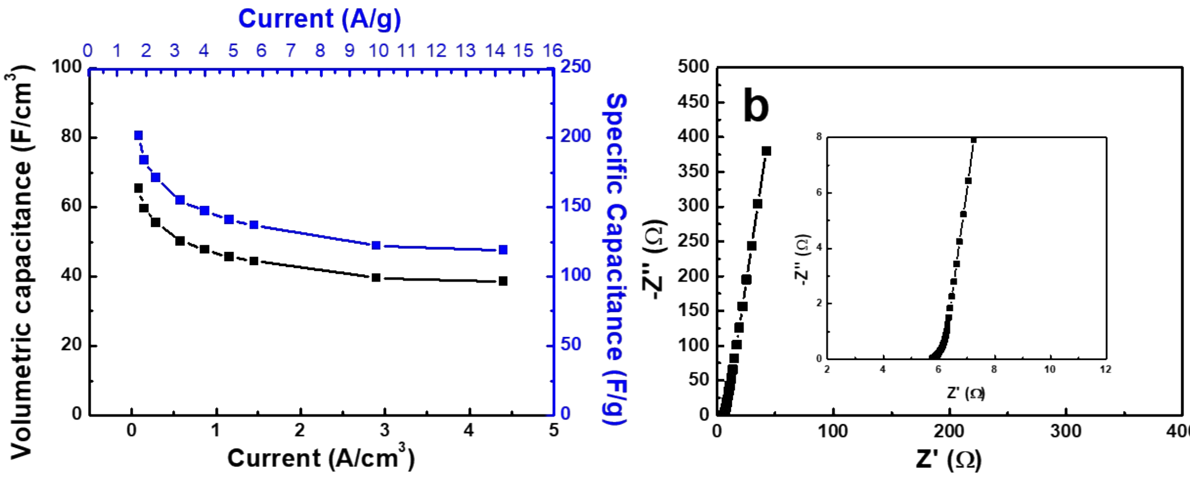


**Figure S9. Electrochemical properties of the symmetric supercapacitor.** (a) Specific and volumetric capacitance of the symmetric supercapacitor at various current values between 0.3 (0.072 A/cm$^3$) to 15 A/g (3.6 A/cm$^3$). (b) Electrochemical impedance spectroscopy (EIS) data of the symmetric supercapacitor over the frequency range from 10 kHz to 0.01 Hz. Inset shows the magnified view for low frequency data.

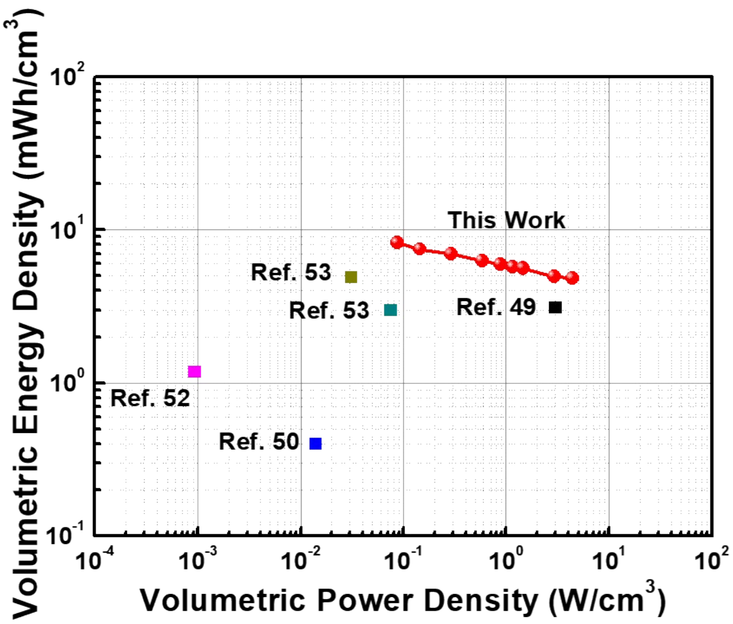


**Figure S10. Ragone Plot comparison of volumetric energy and power density of our symmetric supercapacitor based on NTPPy NWs electrodes and other references.**

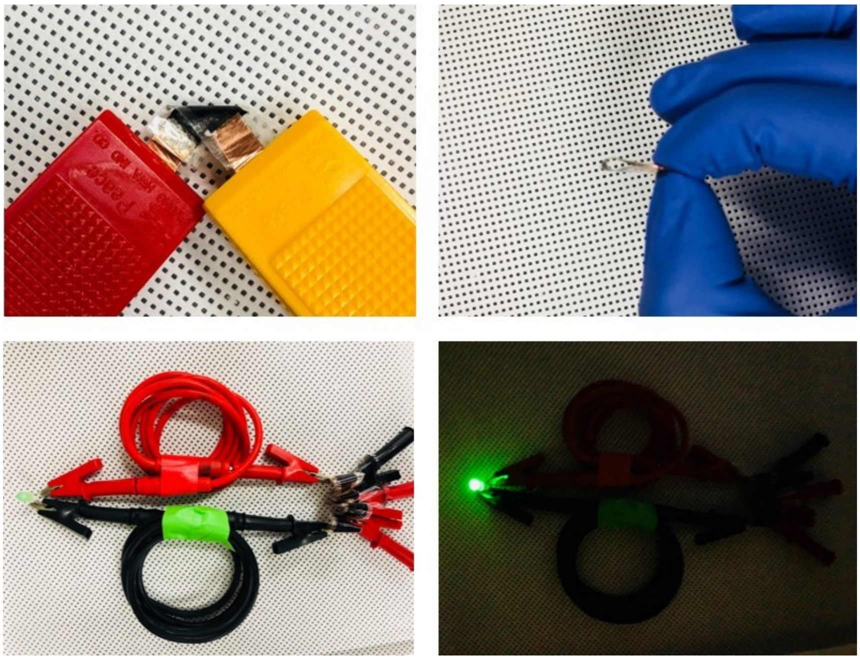

**Figure S11. Optical images showing the flexibility of all-solid-state symmetric supercapacitor based on NTPPy NWs electrodes.**


1. A. V. Dolbin, M. V. Khlistyuck, V. B. Esel'son, V. G. Gavrilko, N. A. Vinnikov, R. M. Basnukaeva, I. Maluenda, W. K. Maser and A. M. Benito, *Appl. Surf. Sci.*, 2016, **361**, 213-220.
2. Z.-D. Huang, B. Zhang, S.-W. Oh, Q.-B. Zheng, X.-Y. Lin, N. Yousefi and J.-K. Kim, *J. Mater. Chem.*, 2012, **22**, 3591-3599.